

High-density Surface EMG: Techniques and Applications at a Motor Unit Level

**DICK F. STEGEMAN^{1,2,*}, BERT U. KLEINE², BERND G. LAPATKI³,
JOHANNES P. VAN DIJK^{1,3}**

¹*Donders Institute for Brain, Cognition and Behaviour, Radboud University Nijmegen, Medical Centre Nijmegen, Nijmegen, The Netherlands*

²*Faculty of Human Movement Sciences, Research Institute MOVE, VU University Amsterdam, The Netherlands*

³*Klinik für Kieferorthopädie und Orthodontie Universitätsklinikum Ulm, Germany*

Surface EMG comprises a variety of widely applied experimental tools in basic neuroscience, biomechanics and exercise physiology, but also in applied disciplines like clinical neurophysiology, ergonomics and sports sciences. To increase the usefulness of surface EMG, we contributed to the introduction and application of a spatiotemporal variant of the usual single channel surface EMG techniques, called high-density surface EMG (HD-sEMG). In the present paper, we first discuss the background of the HD-sEMG technique and basic principles of recording and analysis. In a second part, we illustrate the usefulness of the technique on the basis of studies in which the analysis of HD-sEMG at a motor unit level is at hand. It concerns a precise analysis of the activity of the facial musculature that leads to a map of muscle fibre directions and the positions of motor endplate zones. Two other applications refer to neuromuscular pathology, being motor unit number estimation and the quantification of spontaneous motor unit activity, known as fasciculations.

Key words: high density surface EMG, motor unit number estimation, fasciculations, spatiotemporal EMG activity, facial musculature

1. Introduction

Surface EMG (sEMG) has been used extensively in fundamental motor control studies, in studies related to normal and pathological human movement coordination and it also has wide applications in the clinical neurophysiology supporting for instance

* Correspondence to: Dick F. Stegeman, 920 Department of Neurology / Clinical Neurophysiology, Donders Institute for Brain, Cognition and Behaviour, Radboud University Nijmegen, Medical Centre Nijmegen, P.O. Box 9101, 6500HB Nijmegen, The Netherlands, e-mail: d.stegeman@neuro.umcn.nl
Received 20 March 2012; accepted 24 April 2012

the estimation of nerve conduction variables. However, the judgement of voluntary recruitment of motor units (MUs) and muscle function is regarded to be best possible with intramuscular needle EMG in clinical neurophysiology or with wire EMG as often used in basic motor control studies. This is for good reasons because the close observation of MUs allows relatively easy isolation and recognition of MU firings, whereas the motor unit action potential (MUAP) waveforms contain sensitive markers for pathological processes. An important limitation of routine intramuscular recordings is that electrical events originating in the MU are exclusively measured as a time-varying signal. The same holds for the traditional concept of sEMG with the application of a single pair of electrodes over a muscle as a whole (bipolar sEMG). Any single channel recording misses spatial information, which ignores that muscle electrophysiological activity, like brain activity, certainly is a spatiotemporal signal. This was already recognized by pioneers of needle EMG. With multielectrode needles [1] and by using scanning EMG [2] insight in the spatial profile of the activity within a muscle was obtained.

The possibilities of determining the spatial profiles of surface EMG were already explored in the early 1970's [3]. An advantage of surface EMG over intramuscular EMG, apart from the non-invasiveness and the relative ease to obtain spatial distributions, is its high reproducibility in follow up studies. About fifteen years ago, our group from the University of Nijmegen started with what we called "high-density surface EMG" (HD-sEMG) [4]. This method uses a 2-dimensional (2D) grid comprising many closely spaced electrodes (3–6 mm center-to-center) and generally measures a distribution of activity over a confined area. Such 2D electrode grid principle was



Fig. 1. Electrode grid with 130 electrodes and an interelectrode distance (IED) of 5 mm for use on larger limb muscles. The inset shows a close-up of an electrode. The serrated structure ensures comparatively large contact area, and thus low impedance at a small electrode diameter (from [9])

first described by Masuda et al. [5]. Up to 128 or presently even more channels are in use simultaneously (Fig. 1). Relatively new in our approach at that time was the so-called monopolar recording, facilitating flexible online or off line derivation (see below). The implementation of the technique and our experience with various applications have confronted us with technical challenges, some of which are more difficult to deal with than others. The main elements of HD-sEMG concern the electrode grid, the multichannel amplifier, the signal processing steps and, last but not least, the interpretation and presentation of the large amount of data. In the course of the years, more groups adopted the intrinsic possibilities of HD-sEMG techniques in their basic or clinically oriented research [6–8]. In the next section (“Techniques”) we will illustrate a number of methodological issues with respect to HD-sEMG. In the following section “Applications”, a number of clinically relevant studies will be reviewed. These studies connect to the use of HD-sEMG to evaluate single MU properties and MU firing characteristics.

2. Techniques

2.1. Electrodes

Electrode grid design is one of the challenging aspects of HD-sEMG. There is a clear friction between a number of aspects in the design, best summarized with the four factors: speed of application, comfort for the subject, signals quality and last-but-not-least price. We first adopted a dry electrode principle (Fig. 1, [9]). The single electrodes were adapted from commercially available printed circuit board testing probes (type “serrated contact”; see the inset in the lower right corner of Fig. 1) because of their favourable impedance [10]. They are somewhat uncomfortable during longer use or when used in sensitive areas such as the face. Furthermore, absence of electrode gel may cause less optimal or even failing contacts. Their advantages for sure are a fast application and, related to that, the ease of replacing the grid to find an optimal recording position. More recent grid designs are exemplified in Fig. 2 [11] and Fig. 3 [12]. These electrodes are dependent on a good contact via electrode gel application and can even be used in the more sensitive skin areas even with uneven contours [13]. The disadvantage of these flexible electrode arrays is that their fixation is more time-consuming and that they are less easily to be repositioned. However, signal to noise ratio is improved compared to dry electrodes [11] and these grids can even be used in dynamic conditions.

2.2. Spatial Derivations

We already mentioned the recording of HD-sEMG signals “monopolarly”, i.e. against a far away common reference electrode for all channels. This gives additional information to the regular bipolar recording and facilitates flexibility in online and post-hoc signal processing [14]. Probably because of the high demands to the electronics,

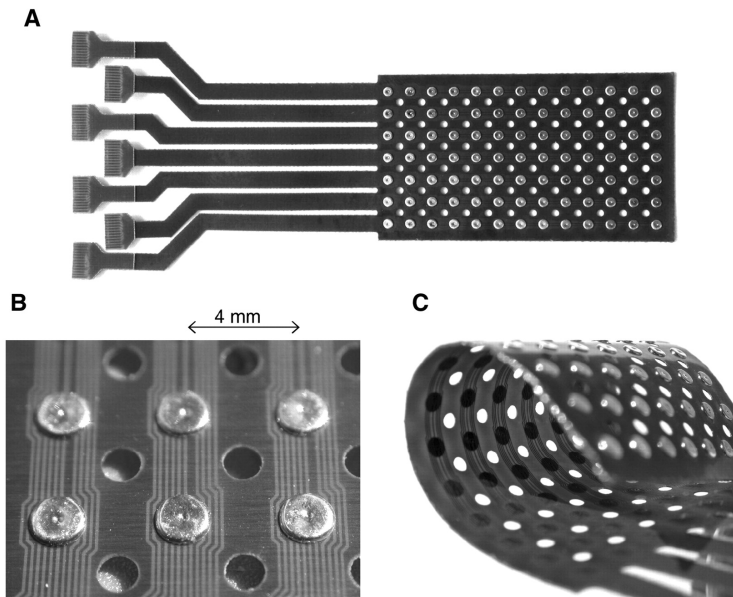


Fig. 2. Part A: photograph of a surface electromyography (sEMG) multielectrode grid manufactured by using flexprint techniques. It consists of 7 x 13 electrodes, with an interelectrode distance of 4 mm. In principle, grids of any desired electrode sizes and arrangements can be manufactured. Part B: each electrode (1.95 mm in diameter) consists of a copper body, which has been surface coated with pure silver (99.99% Ag). Part C: illustration of the high mechanical flexibility of the multielectrode grid. Total thickness of the flexprint (electrode, carrier material, traces, protection lacquer) is 470 μm in the area of the electrodes and 150 μm between them. (from [11])

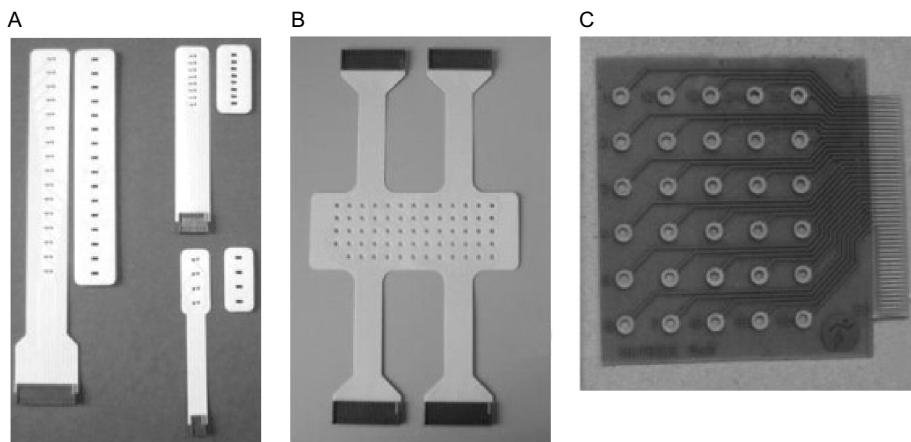


Fig. 3. Part A: Examples of linear electrode arrays with different electrode numbers and interelectrode distances. The cavities in the double adhesive foam are filled with gel, through the holes in the arrays, after positioning. Part B: Example of a two-dimensional flexible electrode grid (LISiN-Spes Medica, Italy) with 64 electrodes. Part C: Printed circuit bi-dimensional electrode array of 6 x 5 electrodes. (adapted from [12] with written permission from Elsevier publishers)

it took some time before this standard way of recording electrophysiology (ECG, EEG) found its way to surface EMG practice (refer to [3] for an exception). These demands are related to the small HD-sEMG electrodes, so that amplifiers have to deal with relative high electrode impedances, combined with large common mode signals (especially power line interference) to the far away reference. By now, such problems can generally be avoided by modern amplifier technology. The advantage of a monopolar derivation is the possibility to spatially filter the signals theoretically by any combination of two or more electrodes. The regular bipolar derivation of sEMG in fibre direction can be considered as the “basic spatial montage”. A variation on the monopolar derivation, borrowed from EEG practice, is the use of a so-called virtual reference being the average potential profile over all electrodes [7]. The theoretical effect of higher order derivations, being practical realizations of first- or higher-order spatial derivatives of the potential profiles, is mainly a modulation of spatial selectivity. In a study of Farina et al. [15], the authors showed the factual influence of different derivations for the tibialis anterior muscle (Fig. 4). Motor unit firings are clearly visible in the longitudinal double differential (LDD) derivation and the lower traces in Fig. 4. The MUAP duration was found to be shorter with LDD and with the 2-D systems than with the other filters. The increase in selectivity with a higher order



Fig. 4. Raw surface EMG signals detected with an electrode grid during a contraction of the tibialis anterior muscle of a single subject (30% MVC contraction level). The signals have been recorded from the central location. Interelectrode distance was 5mm. The signals were obtained by linear combinations of the same monopolar raw signals. The signals are amplitude normalized. S/DD = single and double differential, L = longitudinal. T = transversal. (adapted from [15] with written permission from IEEE publishers)

filtering is visible in an increased separation of the single MU firings. The 2-D filters investigated showed very similar performance and can be considered equivalent from the point of view of spatial selectivity. So, when using a 2-D filtering, a higher order derivation than the well-known Laplacian derivation (indicated as NDD in Fig. 4) does not seem beneficial. From a practical viewpoint that is good news, because increasing the number of electrodes involved in a derivation, increases the risk of including one with a suboptimal skin contact, disturbing the combined signal. One should realize that increasing selectivity with spatial filtering also means a loss of the presence of distant (deep), compared to nearby (superficial), MUs in the EMG signal and thus a decrease of the field-of-view [16]. This has negative consequences for the representativeness of the signal for the muscle studied especially in depth, but works positive for the possibility to decompose the EMG signal in MU contributions (see below) and it decreases the unwanted registration of signals from adjacent muscles (called “cross-talk”).

2.3. Directions of Observation

The obvious advantage of a 2-D grid also is the possibility to observe a muscle’s activity in more directions. Simply stated one can visualize and analyse the propagation of MUAPs in electrode columns along the fibre direction, but one can also observe how MUAPs change in an electrode sequence perpendicular to the fibre direction (Fig. 5). Applications of the first direction were already known from smaller or larger so-called linear array electrodes (Fig. 3A) [17]. An application of the second

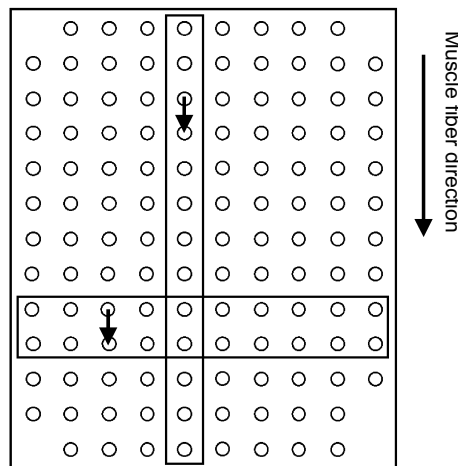


Fig. 5. Schematic representation of an electrode grid. Electrodes are arranged in a 10×13 matrix. Bipolar derivation is mostly obtained by subtracting the signals from two adjacent electrodes in the fiber direction (small arrows). So, the horizontal rectangle then indicates the electrodes needed for a bipolar derivation from rows 9 and 10 (from [22])

was first reported by Monster and Chan (1980) [18] on the relation between MUAP amplitude and MU location. Both orthogonal directions can best be presented in so-called “MUAP fingerprint”. A typical example of such a MUAP fingerprint is shown in Fig. 6 (presenting a biceps brachii MU, not published). As will be illustrated in the following sections, these different directions of observation aim at principally different applications.

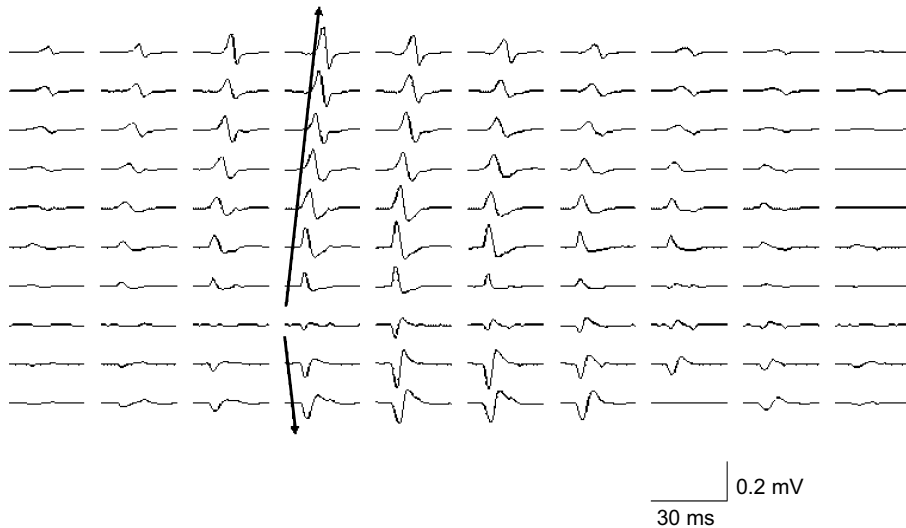


Fig. 6. A motor unit potential fingerprint. It is a 10 x 10 representation of a spike triggered average of the activity of a single motor unit in the biceps brachii muscle (bipolar derivation, IED = 5mm). Clearly visible is the propagation of the action potential away from the motor endplate region (3rd row from the bottom) in two directions vertically in the grid presentation. In the horizontal direction, the decline of the MUAP with increasing distance from the column closest to the underlying motor unit (4th column from the left) is noted

2.4. Muscle Fibre Propagation

The propagation of action potentials which can be observed in fibre direction (Fig. 5, column wise) is mostly summarized by a mean muscle fibre conduction velocity (MFCV). MFCV almost invariably declines during fatigue in isometric contractions if force levels are moderate to maximal. The accumulation of extracellular potassium, especially in the tubuli, and the accumulation of lactate, together with a lowering of the pH, seems to be the main determinants for the change in MFCV. At low force levels an increase of MFCV can be found during long lasting contractions, most likely due to recruitment of new, non-fatigued MUs. The study of MFCV has found its applications in the fields of exercise physiology and rehabilitation, but also in clinically oriented studies [6, 8]. Instead of estimating an average propagation velocity as MFCV, the distinction between different peaks in the EMG signal might reveal

a physiologically relevant distribution of velocities [19]. In that case each peak still may represent a mixture of two or more intermingled MUAPs of closely occurring MU firings. As will be discussed below, certainty on single MUAP behaviour with respect to this velocity behaviour or any other property can only be obtained with a decomposition of the EMG signal into firing characteristics of single MUs.

2.5. Decomposition of the EMG Signal

The ultimate answer to the question of separating an EMG signal in the firing characteristics of all contributing MUs has challenged a wide community of “signal processors” as an ideal typical problem in their field. The first studies used special or conventional intramuscular electrodes [20, 21]. For surface EMG, the use of high density grids appeared to be a great support in the attempts to analyse these non-invasive signals, especially the use of the EMG channels perpendicular to the fibre direction. Crucial in the decomposition of the EMG signal is the identification and classification of the individual MU firings. This can be achieved by using the unique spatial and temporal characteristics of each MU potential recorded with HD-sEMG. In that way, the repeated firing of a specific MU is detected amongst the firing events of the other MUs of which the activity is simultaneously observed. It thus appears that the signals from channels perpendicular to the muscle fibre direction are most informative for identification of the firings of a MU (Fig. 7A, [22]). To obtain the results as those in Fig. 7, the monopolar HD-sEMG signal was spatially filtered by constructing a bipolar derivation and high-pass filtered at 15 Hz to remove movement artefacts. Action potentials were then clustered semi-automatically according to their spatial properties. Templates were constructed (Fig. 7B) and used for template matching after which a complete firing pattern could be deduced [22].

Recent work using advanced statistics such as “blind source separation” made a substantial step forward in the decomposition of the HD-sEMG [23, 24]. Despite such technical improvements, most results obtained using surface EMG are still derived from recordings during relatively low activation levels. At higher levels the interference by the summed activity of different active MUs prohibits reliable identification of individual MUs. On the level that can be reached and the number of electrodes needed to obtain a reliable decomposition result, the published data are not very consistent yet. For instance, Nawab et al. [25] show firing events of up to 40 identified MUs in a 75% MVC activation of the biceps brachii muscle by using only a small (2 cm diameter) 5-pin electrode. Decomposition of signals from such activity level has never been reported by any other research group using HD-sEMG, even with many more electrodes.

The decomposition procedure leads to averaged (i.e., low-noise) fingerprints from the repeated firings of a MU revealing topographical characteristics of this MU. Such MU fingerprints were analysed to topographically characterise the facial musculature [13] and used in hand muscles for improving the method of MU counting [26]. Both

applications will be discussed in the application sections below. Any decomposition result also provides firing characteristics of several MUs. The analysis of such MU discharge sequences contributes to the understanding of the essentials human motor control in health [27] and in disease [28].

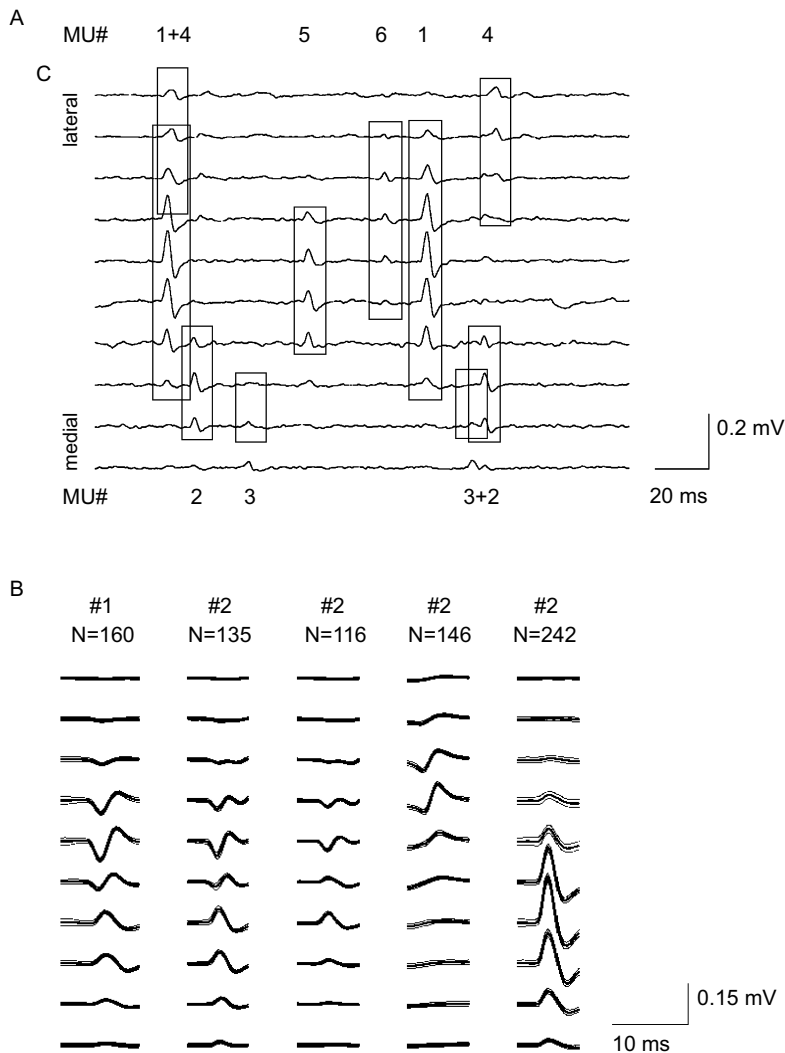


Fig. 7. Two illustrations of the principle of MU decomposition from recordings perpendicular to the muscle fibre direction. Part A: A short segment of raw sEMG from 10 channels measured in the direction perpendicular to the fibres of the biceps brachii muscle. The activity from six different MUs can be observed, partly in overlap with each other. The MUs can relatively easily be discerned because of their specific spatial profile in this direction of observation. Part B: Five different MUAP wave shapes belonging to the vastus lateralis muscle. Part B: Corresponding averaged MUAPs. The firing variability within the clusters is indicated (part B from [22])

3. Applications

3.1. Facial Motor Unit Anatomy and Guidelines for Electrode Placement in Conventional (bipolar) sEMG

Adapted from: PhD-thesis B.G. Lapatki, The Facial Musculature – Characterisation at a Motor Unit Level, 2010 (Lapatki, 2010)

3.1.1. Introduction

The facial musculature is a three-dimensional assembly of multiple small muscle bundles and sheet-like muscle fibre arrays. The independently controlled subcomponents of this complex muscle system are essential for the functioning of the orofacial sense organs and mediate emotional and affective states (mimic expression). Important characteristic anatomical features of the facial muscles are interdigitation and overlap of several muscle subcomponents in relatively small areas (especially in the lower facial area), and high inter- and intra-individual variability in muscle location [29–31].

Until recently, other basic properties of facial MUs, such as their spatial spread and orientation, and the location of the endplate zones, were not specified. HD-sEMG is the obvious method of choice to fill that gap of knowledge.

We conducted a study [13] to systematically determine topographical MU characteristics (i.e. their location, spatial orientation and endplate zone) of the lower facial musculature, and to compare the results to basic anatomical knowledge and data obtained in histo-chemical studies.

3.1.2. Motor Unit Anatomy

Thirteen healthy subjects were specially trained to perform selective contractions of the depressor anguli oris (DAO), depressor labii inferioris (DLI), mentalis (MEN), and orbicularis oris inferior (OOI) muscles. Signals were recorded using flexible HD-sEMG grids as described before. For each subject and each muscle and for different low contraction levels, MU fingerprints were decomposed from the raw sEMG data according their spatio-temporal amplitude characteristics as also described before. Then the lower facial MUs' endplate zones and main muscle fibre orientations were extracted. After applying a spatial warp to correct for the different facial sizes and shapes, results were projected on the individual faces of the subjects. As an example, Fig. 8 shows two monopolar (Figs. 8A and 8B) and two bipolar (Figs. 8C and 8D) MU fingerprints decomposed from data recorded during a 5% MVC contraction of the DAO muscle. Endplate positions and muscle fibre orientations are represented by grey dots and lines, respectively. Other examples are given for the DLI muscle. Here, the data from two representative subjects (Figs. 9A and 9B), demonstrate the occurrence of MU endplates only in the lower portion of the muscle, typically in

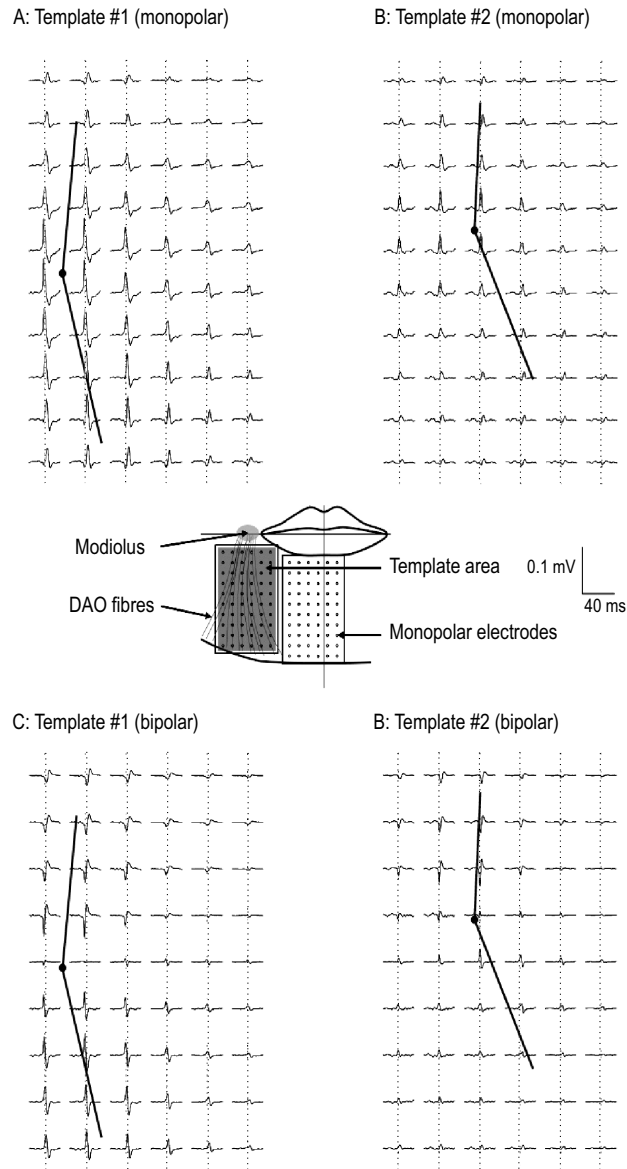


Fig. 8. Parts A, B: Two monopolar and two corresponding bipolar templates showing the spatial amplitude profile of representative depressor anguli oris (DAO) MUAPs and superimposed results of endplate location and main muscle fiber orientation. Only the signals derived from the lateral electrode grid are shown (gray area). MUAPs were decomposed from signals recorded during a 5% maximal voluntary contraction (MVC) of this muscle. Bipolar montages (Parts C and D) were constructed by subtracting the (recorded) monopolar signals of consecutive electrodes in vertical direction. The position of the motor endplate zone can be detected from the bidirectional propagation pattern of the action potentials, which also results in low amplitude at and opposite signal polarity on both sides of the endplate (from [13])

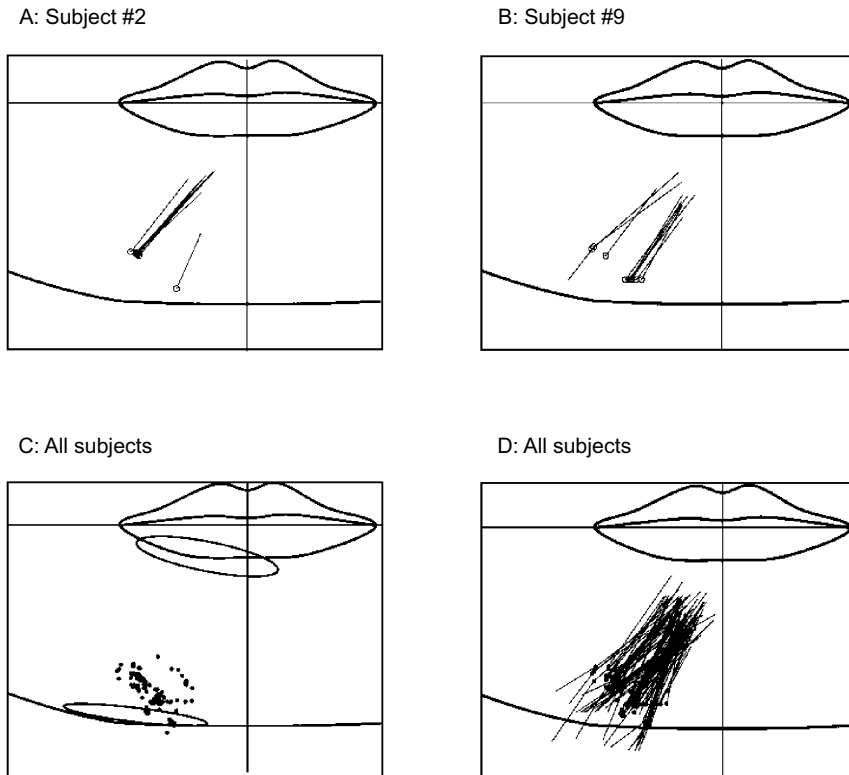


Fig. 9. Depressor labii inferioris (DLI) endplate locations and muscle fiber orientations. Parts A and B: individual data from two subjects showing clustered endplate distribution, i.e., accumulation of endplates in the muscle's lateral and medial portions. Part C: normalised DLI endplate positions of all subjects. In all subjects, DLI endplates were found to lie extremely eccentric between the origin of the muscle at the lower border of the mandibula and its insertion in the lower lip (gray ovals). Part D: normalised DLI fiber orientations of all subjects (from [13])

a lateral and medial cluster. Figure 9C proves that eccentric locations of DLI MU endplates (near the origin of this muscle) were a common finding. Figure 9D shows the fibre orientation of all decomposed DLI MUs which is consistent with illustrations in anatomical textbooks.

This study, published in 2006 [13], revealed a distribution of the lower facial MU endplates in more or less restricted, distinct clusters on the muscle often with eccentric locations. The results add substantially to the basic neurophysiologic and anatomical knowledge of the complex facial muscle system. They can also be used to establish objective guidelines for placement of conventional (surface or needle) EMG electrodes as well as for clinical investigations on neuromuscular diseases affecting the facial musculature.

3.1.3. Guidelines for Optimal Electrode Position

Locations of conventional surface electromyography (sEMG) electrodes in the face are usually chosen on a macro-anatomical basis. However, establishing electrode positioning guidelines is a challenging task. It requires consideration and balancing of several aspects, such as proximity of a proposed electrode site to underlying muscle with minimal intervening tissue, alignment of a bipolar electrode parallel to muscle fibre direction, avoiding that a bipolar electrode is positioned across the MU endplate region, electrode attachment to a proposed site without undue problems e.g. from skin folds or curvatures, and minimising crosstalk from adjacent muscles [32]. Neither anatomical studies, nor electrophysiological investigations with conventional techniques can provide sufficient information regarding all relevant criteria for bipolar electrode placement. HD-sEMG allows filling this gap. We used the collected data described in the previous paragraph to position virtual electrode pairs in the interpolated monopolar MU action potentials at different positions along muscle fibre direction and calculated the bipolar potentials [33]. Electrode sites were determined where maximal bipolar amplitude was achieved.

Figure 10 illustrates for two subjects the endplate zones, muscle fibre orientations and optimal bipolar electrode positions for the DLI muscle. Values for individual MUs as well as intra-individual mean values are given. The optimal recording positions displayed in this particular illustration refer to bipolar electrodes with an inter-electrode distance of 8 mm and detection surfaces of $4 \times 4 \text{ mm}^2$ which are practicable values for facial sEMG [34].

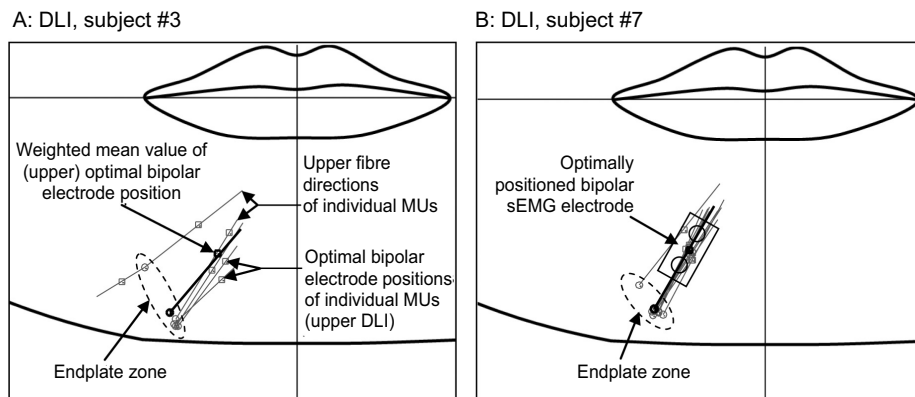


Fig. 10. Endplate zone locations (open circles), muscle fiber orientations (lines), and optimal bipolar electrode positions (open squares: center of bipolar montages) for different motor units (gray); mean values are indicated with corresponding black symbols for the depressor labii inferioris (DLI) muscle. Part A: Results for one subject. Motor unit locations were found to be distributed on two clusters though the lateral cluster consisted of one motor unit only. The bold black square indicates the optimal position for sEMG recordings from the DLI's upper portion in this participant based on maximal amplitude. Part B: Corresponding results for another participant. The rectangle with two open circles depicts an optimally positioned bipolar electrode configuration (from [33])

In principle, this approach can be applied to all musculature accessible to sEMG. We established electrode positioning guidelines for a number of muscles of the lower face. Facial sEMG has proven to be a valuable research and diagnostic tool for applications in psychophysiology, speech physiology and dentistry. The guidelines presented will likely improve the validity and reproducibility of applications in these fields [33].

3.2. Motor Unit Number Estimation

Adapted from: PhD-thesis J.P. van Dijk, On the number of motor units, 2010 (Van Dijk, 2010)

3.2.1. Introduction

In 1971, Alan McComas and co-workers introduced a method to estimate the number of MUs in a muscle [35]. This method is based on the principle that an estimate for the number of MUs can be derived from the quotient of the maximal compound muscle action potential (CMAP) and the mean amplitude size of the MU potentials. This elegant method, known as the incremental counting technique, turned out to have a number of drawbacks, such as the difficulty to recognise small MUAPs, a possible overestimation due to alternating MUAPs, and a limited sample size alternation occurs when two or more MUAPs have a changes of firing not 0 or 1, but somewhere between 0 and 1).

New methods that have emerged differ mainly in the way the mean MUAP is determined [36]. At present, there is no methodology that can practically determine the number of MUs with such an accuracy that allows for validation of the motor unit number estimation (MUNE) techniques. This lack of a “gold-standard” is problematic for two main reasons. First, there is no way of knowing whether a newly developed method actually represents the amount of motoneurons better. Second, it is unknown if a method is biased towards lower or higher numbers. A straight-forward strategy to overcome these problems is choosing the best method based on theoretical grounds and to test this method under practical conditions.

3.2.2. High-density MUNE- a Novel Approach

Recently, we introduced a MUNE technique that uses HD-sEMG because of its theoretical advantages [26]. The advantages of the high-density approach are: 1) MUAPs can more easily be recognized because of the additional spatial information and, to a certain level, alternation can be resolved; 2) A relative large number of MUAPs can be obtained; 3) small MUAPs are more easily recognized because of the small electrodes size, spatial information, and because the optimal position is always covered by the electrode grid; 4) Multiple MUAPs can be obtained from one stimulation site

and, therefore, phase cancellation effects, that also occur in the maximal CMAP, are included; 5) The spatiotemporal difference between the maximal CMAP and the mean MUAP provides an indication of the representativity of the latter. The high-density MUNE method contains elements of the original incremental counting technique [35] and the multiple point stimulation technique [37].

A flexible high-density electrode grid of 8x15 Ag-AgCl electrodes with an interelectrode distance of 4 mm (Fig. 2) was placed over the thenar muscle of the non-dominant hand [11]. The median nerve was stimulated using an electrical constant current stimulator with square pulses of 100 μ s. The MUNE technique has been described in detail before [26]. Briefly, electrical pulses were applied to the nerve at a rate of 1Hz with slowly increasing strength. Alternating MUAPs were recognized and disentangled off-line using the spatio-temporal information. The stimulation electrodes were placed at multiple points along the nerve to increase the sample size of MUAPs used in the MUNE. Three proximal CMAPs were then obtained by supramaximally stimulating the median nerve. After decomposition of the signals, the individual MUAPs were compared to exclude multiple inclusions of the same MUAP.

We found that alternation can be recognized using the spatiotemporal information. Reproducibility in healthy subjects showed a mean coefficient of variation of 15% and an intraclass correlation of 0.88. In our study on 15 healthy subjects, the mean estimated number of MUs was in range with similar techniques (271 +/- 107). The relative large sample size should be beneficial for MUNE accuracy and reproducibility. However, as said, due to the lack of a gold standard, the exact accuracy cannot be given for this or any other MUNE method.

3.2.3. Effect of Small MUAPs on MUNE

One of the drawbacks of the original incremental stimulation technique is the difficulty in detecting small MUAPs. Therefore, we conducted a simulation study to determine the effect of small MUAPs on the MUNE [38]. According to consensus criteria, small MUAPs (negative peak amplitude < 10 μ V) should be omitted from the sample because they may have a disproportionate influence and may increase variability [39]. The amplitude of a MUAP is influenced by a number of factors of which MU size and distance to the electrode are most important. As the high-density electrode grid covers the muscle almost completely, there are always electrodes positioned optimally for a certain MUAP. For this simulation study, MUAPs were used from 8 healthy subjects and from 7 patients with amyotrophic lateral sclerosis (ALS) [26]. In the simulations, all unique single MUAPs obtained were combined in each of the two groups to form a muscle's MUAP population. From the eight healthy subjects we retrieved 208 MUAPs, and 130 MUAPs in total were obtained from the ALS group. It is assumed that by combining all the MUAPs obtained from different subjects, a valid distribution of MUAPs from an individual muscle can be created.

By omitting small MUAPs from the mean MUAP, it was found that the variability hardly decreased. However, a large bias was introduced as in the healthy group up to 27% of the small MUAPs had a negative peak amplitude smaller than $10 \mu\text{V}$ [38]. In ALS, only 12% of the MUAPs were considered small MUAPs. A consequence of omitting the small MUAPs was that the difference between the ALS patients and healthy controls was clearly reduced (Fig. 11). This would result in an underestimation of the disease progression while reproducibility hardly improved. Based on this findings we advise not to follow the consensus criteria and to always also include small MUAPs in the estimate.

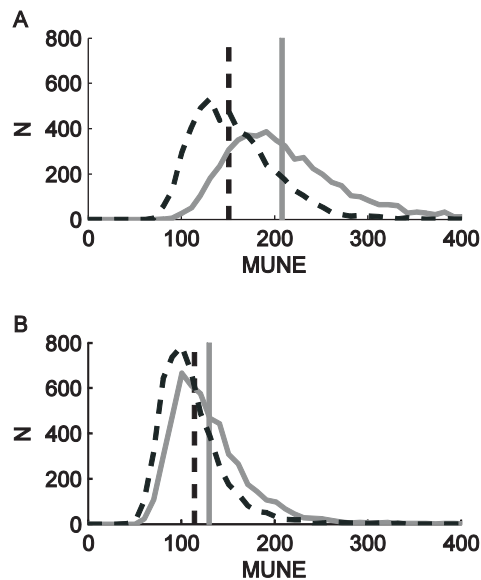


Fig. 11. Distributions of MUNE values at a sample size of 20 samples after repeated simulations with randomly chosen MUAPs (A) from healthy subjects and (B) from MUAPs of ALS patients. The gray distributions result from the entire population of single MUAPs, while the dashed lines are obtained when small MUAPs are omitted. It can be seen that the difference between the healthy distribution and the ALS distribution becomes smaller if small MUAPs are omitted (more overlap between the dashed distributions comparing part A with part B). The gray vertical lines indicate the actual number of MUAPs in the simulation. The dashed vertical lines indicate the number of MUAPs after removal of small ones according to the consensus criteria [39] (from [38])

3.2.4. High-density MUNE in Pathology

Charcot-Marie-Tooth Type-1A

In Charcot-Marie Tooth disease type 1A (CMT1A), weakness is most noticeable in feet and hands while more proximal muscles are much less involved. There is marked phenotypical variability, even between siblings. In a recent study in these patients, we used high-density MUNE to determine, in a cross-sectional design, the number and size of MUs in relation to age [40].

We obtained CMAPs and MUNE values as described above from 69 adult patients with proven CMT1A and from 55 healthy controls. Motor nerve conduction velocity (MNCV) was determined using the place and time difference between proximal and distal CMAP. Muscle strength in the arms was graded according to the Medical Research Council (MRC) scale. Thenar pinch force and functional hand grip were tested using a Martin Vigori-meter [41].

MUNEs and CMAP amplitude values were lower in patients and controls and correlated with hand weakness in patients. CMAP amplitudes declined with age in controls, but not in patients (Fig. 12B). However, MUNE declined in both patients

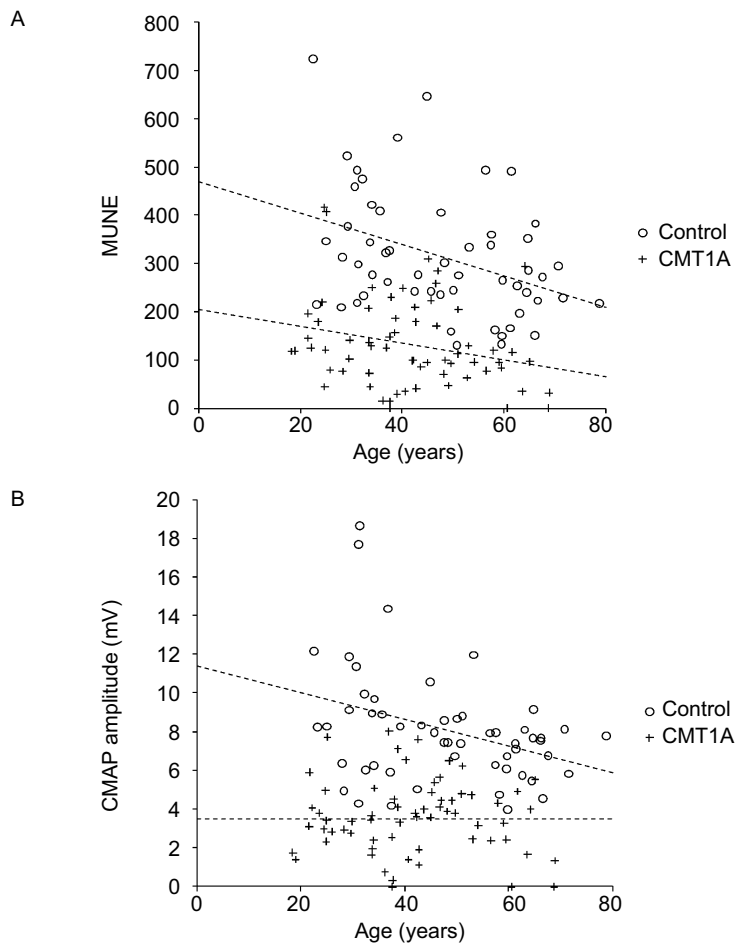


Fig. 12. Part A: Motor unit number estimation (MUNE) versus age for patients with Charcot–Marie–Tooth disease type 1A1A (CMT1A) and controls. The lines represent the significant association between age and MUNE for the control group the patients with CMT1A ($r = 0.25$, $P = 0.046$). Part B: CMAP amplitude versus age for controls and patients with CMT1A. The dotted lines represent the association between age and CMAP amplitude for the healthy controls (significant) and for the patients with CMT1A (non-significant) (from [40])

and controls (Fig. 12A). We found no difference in the observed decline of MUNE between patients and controls. Unexpectedly, we found that MNCV was positively related to age. As this finding contrasts previous reports and MNCV has been found to be related to disease severity, we conclude that a bias may have been present in our data preventing us from drawing firm conclusions. On the other hand, our data are in line with those from the literature suggesting that in CMT1A patients age related MU loss is limited and may be in range of normal aging [42]. As adult patients start-off with a much lower number of MUs, additional loss of MUs due to ageing may affect these patients more than healthy controls with considerable disability as a consequence [40].

Amyotrophic Lateral Sclerosis

In amyotrophic lateral sclerosis (ALS), progressive motoneuron loss is usually observed over a short period of time. ALS patients lose the ability to use their muscles gradually resulting in death in two to three years after diagnosis. To determine if a therapeutic agent is effective, clinical trials are in need for a sensitive marker to monitor disease progression. The most direct and principally unbiased way to monitor motoneuron loss may base on MUNE techniques which could provide such a maker of disease progression. As patients may differ strongly in the rate of disease progression, MUNE might also be used to distinguish between slow and fast progressing patients [43].

We applied high-density MUNE as described above in a follow-up study of 18 ALS patients and followed them for a period of 8 months. For baseline comparison, 26 age-matched healthy subjects were asked to participate in the study as well. Force measurements as hand grip, thenar pinch force and MRC-scale measures of upper limb muscles were obtained. As a clinical outcome measure the ALS functional rating scale (ALSFERS) was obtained as well.

The mean (\pm SD) MUNE was significantly lower in the patients with ALS than in the controls (patients 158 ± 103 versus controls 256 ± 85). MUNE reproducibility was assessed within 2 weeks in 17 ALS patients. MUNE reproducibility was good with an ICC=0.86 and a median CoV of 13.7%. No significant difference was found between test-retest values for MUNE or CMAP amplitude. The reproducibility was similar in patients and controls. All variables, except for the thenar pinch strength test (MVTP), declined significantly over 4 months (Fig. 13). Over 8 months, the MUNE decreased the most (49%) of all variables measured. Moreover, the MUNE decreased significantly more than the CMAP. At 4 months, the decrease in MUNE was already significantly different from the decrease in ALSFRS score.

We think that MUNE might prove to be especially useful in (smaller) phase II clinical trials because these trials need a sensitive efficacy measure early in the disease course [44]. The relatively time-consuming nature of MUNE measurements (compared with other measures, such as the ALSFRS) make them less suitable for large phase III trials.

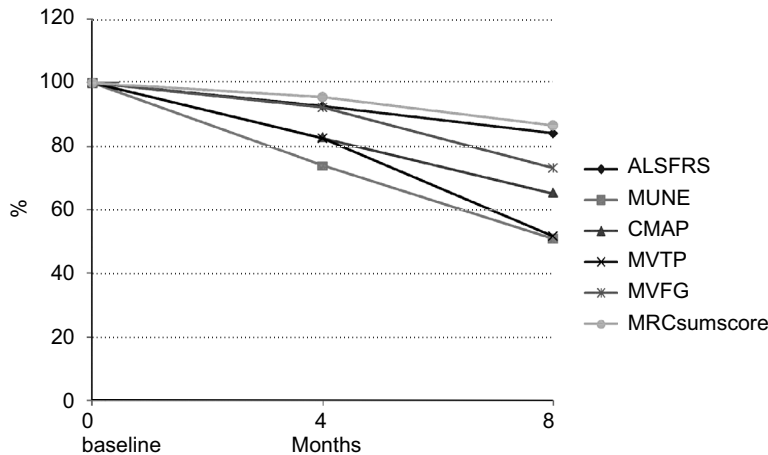


Fig. 13. Percent change in HD-sEMG motor unit number estimate (MUNE), Martin vigorimeter thenar pinch (MVTP), compound muscle action potential (CMAP), Martin vigorimeter functional grip strength (MVFG), ALS functional rating scale (ALSFRS), and MRC sum-score at 4 and 8 months after baseline in a group of 18 ALS patients. Values were normalised to the baseline (at average 1.7 years after first symptoms) (from [43])

3.3. Fasciculations in ALS

Adapted from: PhD-thesis B.U. Kleine, Motor unit discharges- Physiological and diagnostic studies in ALS, Kleine, 2011)

3.3.1. Introduction

Fasciculation is a clinical hallmark of ALS and can be defined as random, spontaneous twitching of a group of muscle fibres belonging to a single MU [45]. Fasciculations can be observed on inspection or palpation of the muscle, but dynamic ultrasound appears to be the most sensitive method [46–48]. With needle or surface electrodes fasciculation potentials (FPs) can be recorded from the resting or active muscle. Although the origin of fasciculations in terms of anatomic localisation has been studied for almost a century, the origin of fasciculations in ALS is still under debate. We hypothesized that the discharge pattern of FPs would be different for FPs arising in the motor axon or in the spinal motor neuron [28].

3.3.2. Firing Pattern of Fasciculations in ALS: Evidence for Axonal and Neuronal Origin

FPs were recorded by HD-sEMG of the biceps brachii or vastus lateralis muscle for 15 minutes in 10 patients with ALS. Records were decomposed into different FP waveforms and their firing moments. The algorithm for MU decomposition shortly described above [22] was adapted for long-duration recordings and for discrimination

of different FPs. The result of automatic full decomposition was checked visually for all firing events. Interspike interval (ISI) histograms were constructed for FPs that fired more than 100 times. The rationale was that peaks in the ISI histogram correspond to a depolarization that brings the membrane close to the threshold for a new FP.

In the patients with ALS, two distinct types of ISI histograms were found, reflecting the origin of fasciculations either in the axonal membrane (Fig. 14A-C) or in the motor neuron itself (Fig. 14D-F) [28]. Some FPs with an axonal origin showed preferential discharge with an ISI of 5 ms (Fig. 14B), which is readily explained by increased super-excitability known from peripheral nerve excitability studies [49]. Because of the analogy between ISI analysis and the recovery cycle, our data support the concept that a large part of ALS fasciculations results from an acquired channelopathy with increased sodium and decreased potassium conductances [50, 51]. A recent study by Mills [52] confirmed the findings on short ISIs.

3.3.3. Fasciculations and Their F-response

We collected firings from the axonal type of FPs. Some of them, probably even the majority, must have originated in the intramuscular arborisation of the motor axon. An action potential that arises distally propagates to all of the MU's muscle fibres, but also antidromically to the motor neuron [53]. Therefore, an F-response is expected to occur after some of the FPs [54]. An FP and its F-response have almost identical spatiotemporal properties and an ISI that corresponds to the length of the nerve. In the ISI histograms from patients with ALS (Fig. 14) no peak attributable to F-responses was found. By chance, we observed FPs with an F-response in a patient that turned out to have benign fasciculations. Therefore, we systematically searched for and found F-responses in recordings from patients with ALS and from patients with benign fasciculations. The stable recoding of HD-sEMG was again essential in that search. It appeared that in both groups and also in healthy subjects FPs with F-response can be recorded [55]. The discrepancy between these results and the results presented in Figure 14 may be explained by the hypothesis that a MU fasciculating at a high rate (required to create Fig. 14) is unable to produce F-responses. Such a hypothesis requires that hyperexcitability of the distal axon is associated with changes in the motor neuron precluding back-firing of F-responses. Another hypothesis is that the axonal fasciculations then arise proximally, probably at the axon hillock. To resolve this question, longitudinal tracking of a MU [56] with fasciculations through different stages of the disease, excitability testing of the FP, or paired pulse F-responses may be useful. HD-sEMG is certainly suitable or even required (MU tracking) in this kind of studies. In any case, the occurrence of FPs with F-responses in a benign condition suggests that ectopic discharges from the distal axon are not a marker of progressive neurodegeneration [55].

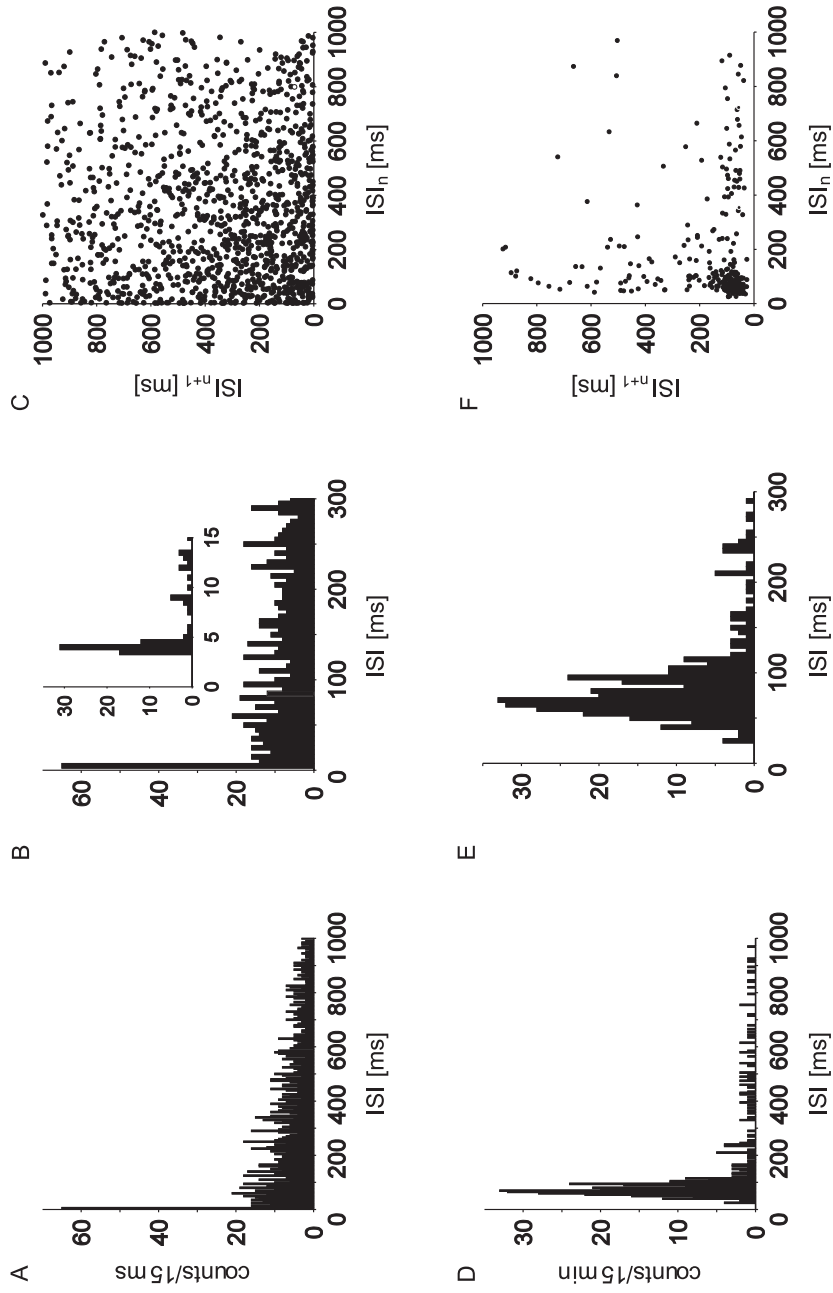


Fig. 14. Firing patterns of two different types of fasciculation potentials (FPs; Parts A–C and parts D–F) that were simultaneously active in the same recording. The interspike interval histogram is plotted at two different resolutions (Parts A, D and parts B, E). The upper (axonal type) FPs show increased firing probability around 4.5 ms (inset in part B). The lower (spinal motor neuron) type of FPs had a longer refractory period (25 ms) and maximum firing probability around 70 msec. Note the absence of a serial correlation in the joint ISI plot (Parts C, F) for both FPs (from [28])

4. Conclusions

High-density surface EMG grids and software tools enable the measurements of MUAP properties and motor unit numbers. Physiological and topographical information becomes available that certainly is beyond the reach of needle EMG. We showed a number of prominent examples from our own research. Common to the three different applications is the decomposition of the signal into the contribution of the underlying MUAPs. Depending on the application, the focus can be on the MUAP and its relation with muscle anatomy or on the discharge pattern and its relation with motor neuron physiology.

Obviously, more could have been illustrated with respect to the use of HD-sEMG. This includes muscle fiber conduction velocity in fatigue and neuromuscular pathology, endplate localization for optimizing botuline toxin injections, the study of normal and abnormal distributions of muscle activation, and muscle fibre propagation disturbances. All of these examples exploit the unique spatial amplitude distribution of MUAPs or sEMG patterns over the skin. Thus, multichannel sEMG provides both classic and new information regarding the neuromuscular system in health and disease. Its main advantage lies in the non-invasive contribution of detailed spatial information to our view of the peripheral part of the human motor system.

Acknowledgment

Discussions with Joleen Blok, Gea Drost, Machiel Zwarts and Mark Massa were greatly acknowledged. The development of the high-density surface EMG system was made possible by a grant from The Technology Foundation STW, Utrecht, The Netherlands (grant NGN 3818). The MUNE study was financially supported by the Prinses Beatrix Fonds grant no. MAR03-0102. The study on fasciculations was financially supported by ZonMw (CZ AGIKO stipendium 940-37-034).

The study on the facial musculature was financially supported by a scholarship of the Deutsche Gesellschaft für Kieferorthopädie (DGKfo), by the Stichting FSHD (Wassenaar, The Netherlands), and by the Department of Neurology (Radboud University Nijmegen Medical Centre).

References

1. Buchthal F., Guld C., Rosenfalck F.: Multielectrode study of the territory of a motor unit. *Acta Physiologica Scandinavica* 1957, 39, 83–104.
2. Stalberg E.: Single fiber EMG, macro EMG, and scanning EMG. New ways of looking at the motor unit. *CRC critical reviews in clinical neurobiology* 1986, 2, 125–167.
3. Gydikov A., Kosarov D.: The influence of various factors on the shape of the myopotentials in using monopolar electrodes. *Electromyography and clinical neurophysiology* 1973, 13, 319–343.
4. Zwarts M.J., Stegeman D.F.: Multichannel surface EMG: basic aspects and clinical utility. *Muscle Nerve* 2003, 28, 1–17.

5. Masuda T., Miyano H., Sadoyama T.: The propagation of motor unit action potential and the location of neuromuscular junction investigated by surface electrode arrays. *Electroencephalogr. Clin. Neurophysiol.* 1983, 55, 594–600.
6. Drost G., Stegeman D.F., van Engelen B.G., Zwarts M.J.: Clinical applications of high-density surface EMG: a systematic review. *J. Electromyogr. Kinesiol.* 2006, 16, 586–602.
7. Merletti R., Avenaggiato M., Botter A., Holobar A., Marateb H., Vieira T.M.: Advances in surface EMG: recent progress in detection and processing techniques. *Critical reviews in biomedical engineering* 2010, 38, 305–345.
8. Merletti R., Botter A., Cescon C., Minetto M.A., Vieira T.M.: Advances in surface EMG: recent progress in clinical research applications. *Critical reviews in biomedical engineering* 2010, 38, 347–379.
9. Blok J.H., van Dijk J.P., Drost G., Zwarts M.J., Stegeman D.F.: A high-density multichannel surface electromyography system for the characterization of single motor units. *Review of Scientific Instruments* 2002, 73, 1887–1897.
10. Blok J.H., Van Asselt S., Van Dijk J.P., Stegeman D.F.: On an optimal pasteless electrode to skin interface in surface EMG. In: Hermens H.J., Merletti R., Rix R., Freriks B. /Eds/. *The state of the art in sensors and sensor placement procedures for surface electromyography European concerted action (BIOMED II, SENIAM, Deliverable 5)*. Enschede: Roessingh Research and Development, 1998, 71–77.
11. Lapatki B.G., van Dijk J.P., Jonas I.E., Zwarts M.J., Stegeman D.F.: A thin, flexible multielectrode grid for high-density surface EMG. *J. Appl. Physiol.* 2004, 96, 327–336.
12. Merletti R., Botter A., Troiano A., Merlo E., Minetto M.A.: Technology and instrumentation for detection and conditioning of the surface electromyographic signal: state of the art. *Clinical biomechanics (Bristol, Avon)* 2009, 24, 122–134.
13. Lapatki B.G., Oostenveld R., van Dijk J.P., Jonas I.E., Zwarts M.J., Stegeman D.F.: Topographical characteristics of motor units of the lower facial musculature revealed by means of high-density surface EMG. *J. Neurophysiol.* 2006, 95, 342–354.
14. Roeleveld K., Stegeman D.F., Vingerhoets H.M., Van Oosterom A.: The motor unit potential distribution over the skin surface and its use in estimating the motor unit location. *Acta Physiol. Scand.* 1997, 161, 465–472.
15. Farina D., Arendt-Nielsen L., Merletti R., Indino B., Graven-Nielsen T.: Selectivity of spatial filters for surface EMG detection from the tibialis anterior muscle. *IEEE Trans. Biomed. Engin.* 2003, 50, 354–364.
16. Staudenmann D., Roeleveld K., Stegeman D.F., van Dieen J.H.: Methodological aspects of SEMG recordings for force estimation – a tutorial and review. *J. Electromyogr. Kinesiol.* 2010, 20, 375–387.
17. Merletti R., Farina D., Gazzoni M.: The linear electrode array: a useful tool with many applications. *J. Electromyogr. Kinesiol.* 2003, 13, 37–47.
18. Monster A.W., Chan H.: Surface electromyogram potentials of motor units; relationship between potential size and unit location in a large human skeletal muscles. *Experimental Neurology* 1980, 67, 280–297.
19. Houtman C.J., Stegeman D.F., van Dijk J.P., Zwarts M.J.: Changes in muscle fiber conduction velocity indicate recruitment of distinct motor unit populations. *J. Appl. Physiol.* 2003, 95, 1045–1054.
20. De Luca C.J., Forrest W.J.: An electrode for recording single motor unit activity during strong muscle contractions. *IEEE Trans. Biomed. Engin.* 1972, 19, 367–372.
21. McGill K.C., Cummins K.L., Dorfman L.J.: Automatic decomposition of the clinical electromyogram. *IEEE Trans. Biomed. Engin.* 1985, 32, 470–477.
22. Kleine BU, van Dijk JP, Lapatki BG, Zwarts MJ, Stegeman DF: Using two-dimensional spatial information in decomposition of surface EMG signals. *J. Electromyogr. Kinesiol.* 2007, 17, 535–548.
23. Holobar A., Farina D., Gazzoni M., Merletti R., Zazula D.: Estimating motor unit discharge patterns from high-density surface electromyogram. *Clin. Neurophysiol.* 2009, 120, 551–562.

24. Holobar A., Minetto M.A., Botter A., Negro F., Farina D.: Experimental analysis of accuracy in the identification of motor unit spike trains from high-density surface EMG. *IEEE Trans. Neural. Syst. Rehabil. Eng.* 2010, 18, 221–229.
25. Nawab S.H., Chang S.S., De Luca C.J.: High-yield decomposition of surface EMG signals. *Clin. Neurophysiol.* 2010, 121, 1602–1615.
26. van Dijk J.P., Blok J.H., Lapatki B.G., van Schaik I.N., Zwarts M.J., Stegeman D.F.: Motor unit number estimation using high-density surface electromyography. *Clin. Neurophysiol.* 2008, 119, 33–42.
27. Negro F., Holobar A., Farina D.: Fluctuations in isometric muscle force can be described by one linear projection of low-frequency components of motor unit discharge rates. *The Journal of Physiology* 2009, 587, 5925–5938.
28. Kleine B.U., Stegeman D.F., Schelhaas H.J., Zwarts M.J.: Firing pattern of fasciculations in ALS: evidence for axonal and neuronal origin. *Neurology* 2008, 70, 353–359.
29. Blair C., Smith A.: EMG recording in human lip muscles: can single muscles be isolated? *Journal of Speech and Hearing Research* 1986, 29, 256–266.
30. Kennedy J.G., Abbs J.H.: Anatomic studies of the perioral motor system: foundations for the studies in speech physiology. New York, Academic Press, 1979.
31. Salmons S.: Muscle. In: Williams PL, ed. *Gray's Anatomy. The anatomic basis of medicine and surgery*, 38 ed. New York: Churchill Livingstone, 1995.
32. Fridlund A.J., Cacioppo J.T.: Guidelines for human electromyographic research. *Psychophysiology* 1986, 23, 567–589.
33. Lapatki B.G., Oostenveld R., Van Dijk J.P., Jonas I.E., Zwarts M.J., Stegeman D.F.: Optimal placement of bipolar surface EMG electrodes in the face based on single motor unit analysis. *Psychophysiology* 2010, 47, 299–314.
34. Zwarts M.J., Lapatki B.G., Kleine B.U., Stegeman D.F.: Surface EMG: how far can you go? *Suppl. Clin. Neurophysiol.* 2004, 57, 111–119.
35. McComas A.J., Fawcett P.R., Campbell M.J., Sica R.E.: Electrophysiological estimation of the number of motor units within a human muscle. *J. Neurol. Neurosurg. Psychiatry* 1971, 34, 121–131.
36. Shefner J.M.: Motor unit number estimation in human neurological diseases and animal models. *Clin. Neurophysiol.* 2001, 112, 955–964.
37. Kadrie H.A., Yates S.K., Milner-Brown H.S., Brown W.F.: Multiple point electrical stimulation of ulnar and median nerves. *J. Neurol. Neurosurg. Psychiatry* 1976, 39, 973–985.
38. van Dijk JP, Zwarts MJ, Schelhaas HJ, Stegeman DF: Effect of small motor unit potentials on the motor unit number estimate. *Muscle Nerve* 2008, 38, 887–892.
39. Bromberg M.B.: *Motor Unit Number Estimation*: Amsterdam: Elsevier, 2003.
40. van Dijk J.P., Verhamme C., van S.I. et al.: Age-related changes in motor unit number estimates in adult patients with Charcot-Marie-Tooth type 1A. *Eur. J. Neurol.* 2010, 17, 1098–1104.
41. Merkies I.S., Schmitz P.I., Samijn J.P., Meche F.G., Toyka K.V., van Doorn P.A.: Assessing grip strength in healthy individuals and patients with immune-mediated polyneuropathies. *Muscle Nerve* 2000, 23, 1393–1401.
42. Verhamme C., van Schaik I.N., Koelman J.H., de Haan R.J., de Visser M.: The natural history of Charcot-Marie-Tooth type 1A in adults: a 5-year follow-up study. *Brain* 2009, 132, 3252–3262.
43. van Dijk J.P., Schelhaas H.J., van S.I., Janssen H.M., Stegeman D.F., Zwarts M.J.: Monitoring disease progression using high-density motor unit number estimation in amyotrophic lateral sclerosis. *Muscle Nerve* 2010, 42, 239–244.
44. Schoenfeld D.A., Cudkovicz M.: Design of phase II ALS clinical trials. *Amyotroph. Lateral. Scler.* 2008, 9, 16–23.
45. American Association of Electrodiagnostic Medicine glossary of terms in electrodiagnostic medicine. *Muscle Nerve* 2001, Suppl. 10, S1–50.

46. Pillen S., Arts I.M., Zwarts M.J.: Muscle ultrasound in neuromuscular disorders. *Muscle Nerve* 2008, 37, 679–693.
47. Scheel A.K., Toepfer M., Kunkel M., Finkenstaedt M., Reimers C.D.: Ultrasonographic assessment of the prevalence of fasciculations in lesions of the peripheral nervous system. *J. Neuroimaging* 1997, 7, 23–27.
48. Wenzel S., Herrendorf G., Scheel A., Kurth C., Steinhoff B.J., Reimers C.D.: Surface EMG and myosonography in the detection of fasciculations: a comparative study. *J. Neuroimaging* 1998, 8, 148–154.
49. Burke D., Kiernan M.C., Bostock H.: Excitability of human axons. *Clin. Neurophysiol.* 2001, 112, 1575–1585.
50. Kanai K., Kuwabara S., Misawa S., et al.: Altered axonal excitability properties in amyotrophic lateral sclerosis: impaired potassium channel function related to disease stage. *Brain* 2006, 129, 953–962.
51. Vucic S., Kiernan M.C.: Axonal excitability properties in amyotrophic lateral sclerosis. *Clin. Neurophysiol.* 2006, 117, 1458–1466.
52. Mills K.R.: Characteristics of fasciculations in amyotrophic lateral sclerosis and the benign fasciculation syndrome. *Brain* 2010, 133, 3458–3469.
53. Roth G.: The origin of fasciculations. *Ann. Neurol.* 1982, 12, 542–547.
54. Roth G.: Fasciculations and their F-response. Localisation of their axonal origin. *Journal of the neurological sciences* 1984, 63, 299–306.
55. Kleine B.U., Boekestein W.A., Arts I.M., Zwarts M.J., Jurgen Schelhaas H., Stegeman D.F.: Fasciculations and their F-response revisited: High-density surface EMG in ALS and benign fasciculations. *Clin. Neurophysiol.* 2011.
56. Maathuis E.M., Drenthen J., van Dijk J.P., Visser G.H., Blok J.H.: Motor unit tracking with high-density surface EMG. *J. Electromyogr. Kinesiol.* 2008, 18, 920–930.